JOURNAL OF APPLIED POLYMER SCIENCE VOL. 14, PP. 1477-1489 (1970)

Combined Stress Failure Tests for a Glassy Plastic

L. J. BROUTMAN, S. M. KRISHNAKUMAR, and P. K. MALLICK,
Department of Mechanics, Illinois Institute of Technology, Chicago, Illinois 60616

Synopsis

The development of a unique test method for biaxial stress experiments on brittle material is discussed. Results of biaxial tension-tension and tension-compression experiments on poly-methylmethacrylate (plexiglas) are presented. The strength results compare reasonably well with modified distortion energy theory in the tension-compression stress quadrant.

INTRODUCTION

The mechanical properties and theories of fracture of polymeric materials under combined states of stress are important for the design of modern engineering structures and components. Several investigators have shown that the combined stress-fracture strength of brittle materials cannot be predicted with reasonable accuracy from the existing fracture criteria. The experimental data available for different materials do not always fit the same theories of failure. The apparent discrepancies between the theories and experiments occur since the theories are not based on exact conditions of fracture and the early experiments did not consider enough combined states of stress to adequately describe a failure envelope. Furthermore, the specimens and techniques of loading were not sufficient to attain satisfactory results.

In this study, a unique test method has been developed to create an unlimited number of stress states in the tension–tension and tension–compression quadrants. The equipment developed has been used to determine the failure envelope for a poly(methyl methacrylate) (Plexiglas) using cast tubes for test specimens.

Ely[1] investigated the combined stress properties of acrylic tube specimens. The experimental results appear to fit the Stassi law. The strength of acrylic tubes under biaxial stresses was influenced by the rate of loading or time of tests. The experimental techniques developed in this study were quite different than those used by Ely and offer the advantage of simplicity in equipment and technique.

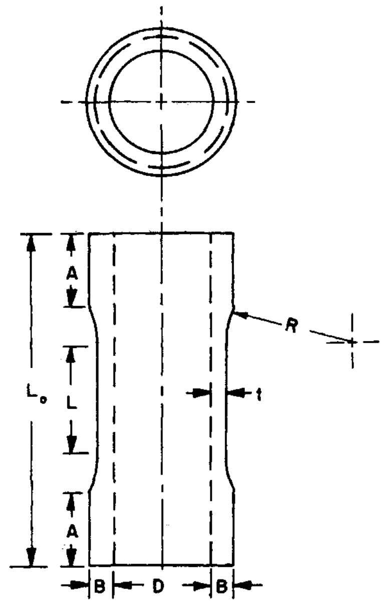

Fig. 1. Plexiglas tube specimen for combined stress tests. Ends machined flat and parallel; concentricity = ±0.004 in.; D = 1.75 in.; t = 0.125 in.; B = 0.25 in.; R = 3.00 in.; L_0 = 7.75 in.; L = 2.04 in.; A = 2.00 in.

TEST METHOD AND SPECIMEN DESIGN

The test method to obtain combined stress states includes the pressurization of thin-walled cylindrical tube specimens (closed end) by various combinations of internal and external fluid pressures. In the conventional end-loading methods, to achieve a tensile or compressive stress, perfect alignment is required for brittle materials. Also frictional forces arise between the specimen ends and end plates when specimens are end loaded for compressive states of stress. These two problems were eliminated by using combinations of internal and external pressures.

Uniaxial tension tests are of the ring-burst type. The internal pressurization of a ring creates a hoop tensile stress in the wall of the ring specimen. This method eliminated the errors that can be caused by the gripping encountered in standard tensile tests. Also, the simplicity of the setup and specimen configuration, the self-aligning feature and simple stress field make the ring-burst tests least likely to produce erroneous results.

The specimens used for biaxial stress experiments were cylinders with a reduced section at the gauge (test) area. The reduced section was used to ensure the initiation of fracture in a uniform wall section away from the bonded specimen ends. The specimen geometry is shown in Figure 1. The specimen dimensions were chosen such that the following conditions exist:

(1) The D/t ratio is large enough so that the radial stress is small compared to the hoop and axial stresses in the wall.

(2) Gauge length L is large enough so that the extraneous stresses developed at the ends would be minimized at the center of the specimen and a uniform stress state would thus exist in the center region.

(3) The fillet radius R is large so that the stress concentration is reduced at the ends of the gauge section.

(4) The B/t ratio is great enough so that the fracture of the specimen somewhere within the gauge section is further assured.

(5) The length of the thicker section of the specimen, A, is large enough so that the bond between the specimen and the end plugs can resist the applied forces.

(6) Minimum manufacturing cost and maximum reproducibility.

The final specimen geometry was developed from preliminary experiments using tubular specimens with varying geometry. The final specimen design was chosen to ensure that the tubes fractured close to the center of the gauge section.

EQUIPMENT DESIGN

For combined stress-fracture experiments, it is desirable to achieve failure by a constant rate of pressure increase. A pressurization system has been designed to provide pressures from 0 to 10,000 psi. The pressure can be increased or decreased at a constant rate with time and can be adjusted anywhere within the range of 0 and 10,000 psi. The rate of pressurization used here was 5000 psi/min. It basically consists of a hydraulic pump and valve units, an electronic control system, and a 4:1 hydraulic pressure intensifier. A double solenoid-operated four-way valve controls the advance, retraction, and idling of the intensifier. Electronic control unit consists of an electroilic valve driver, an amplifier and ramp generator, a ramp-control potentiometer, and a pressure-command potentiometer generates a voltage proportional to the desired maximum pressure. The ramp generator circuit accepts the voltage and ramps its output to the same voltage at a rate determined by the ramp-control potentiometer. The voltage thus obtained is converted to a current suitable to drive the electroilic valve. A relief valve in the line limits the maximum pressure generated by the pump to 2850 psi. A needle valve provided on the inlet side of the intensifier controls the flow and eliminates the shock produced by the fracture of the test specimen.

The equipment designed and constructed for measuring the tensile strength of Plexiglas is shown in Figure 2. Such equipment for tensile tests of brittle materials was first designed by Sedlacek and Halden.[2] The hoop tensile stress is created by the internal pressurization of open-ended rings (Fig. 3) with unrestrained ends.

The equipment consists of two 7-in. diameter platens with a conical cavity in the upper platen and a hemispherical cavity in the lower one.

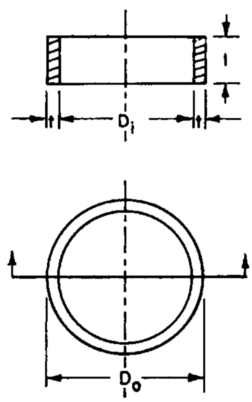

Fig. 2. Plexiglas ring specimen for uniaxial hoop tension tests. Ends machined flat and parallel: D_i = 1.75 in.; D_o = 2.25 in.; t = 0.25 in.; $l = 1.00^{+.000}_{-.001}$ in.

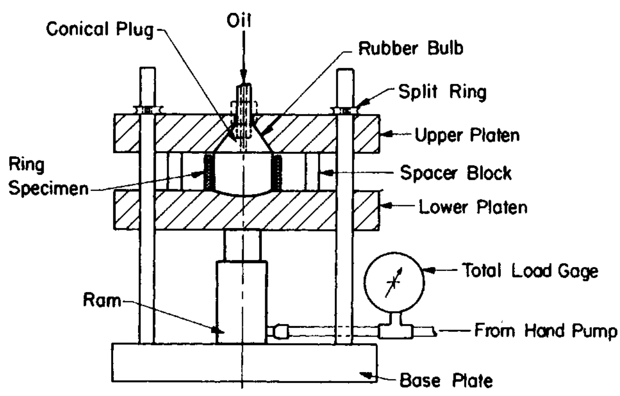

Fig. 3. Tensile test equipment.

The conical cavity opens to the outside and a conical plug with small hole can fit in it. The pressure is applied radially to the ring specimen through a rubber bulb. The conical end of the rubber bulb is squeezed between the conical cavity and the plug to form a leak-proof seal. Three spacer blocks, 2 to 3 mils higher than the ring specimen, are placed around it to ensure that there is no axial restraint on the specimen and that, when the pressure is applied, the specimen can actually float to find its own unrestrained position. The equipment designed does not have to be used with a hydraulic press to clamp the platens but has all these features combined in it.

A pressure vessel has been designed and constructed to provide various combined states of stress in the walls of the tubular specimens. The diagram of the pressure vessel is shown in Figure 4. The vessel was designed for an internal pressure of approximately 15,000 psi. The vessel has an internal diameter of 4.375 in., wall thickness of 1.062 in., and length of 10.5 in. One unique feature of the pressure vessel design is that an unlimited

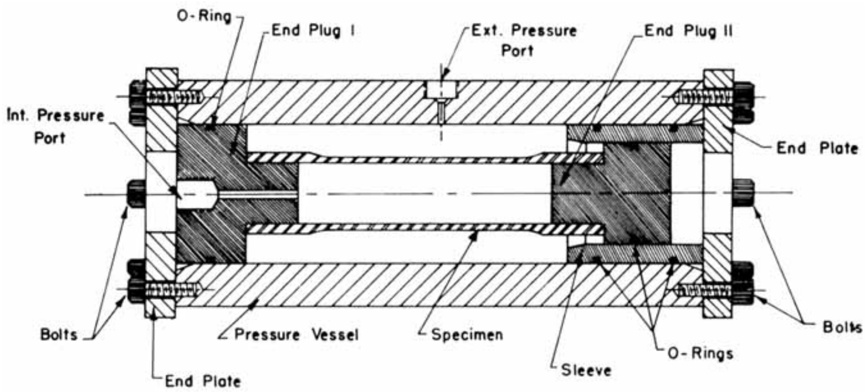

Fig. 4. Pressure vessel for combined stress experiments.

number of stress ratios, both in the tension–tension and tension–compression stress quardrants, can be created in one vessel. This is accomplished by changing the effective area on which the pressure acts in the axial direction. The effective area is changed by changing the size of the end plug on one side of the specimen (end plug II in Fig. 4) and using the corresponding sleeve. Proper O-ring seals are necessary for static sealing. When the pressure is applied, the specimen moves to one side of the pressure vessel (side of the end plug I in Fig. 4) due to pressure acting on a larger area (rim) and rests against the end plate. The effective area on which the pressure now acts in the axial direction is the area (rim) of the end plug II, which remains inserted in the sleeve. This allows the specimen to deflect through one O-ring seal only.

STRESS RATIOS

Various stress ratios used in the combined stress experiments with Plexiglas and the corresponding end plug dimensions (end plug II) are listed in Table I. Lame's equations for thick-walled cylinders[3] were used to calculate the axial and hoop stresses produced in the walls of the test specimens. Figure 5 shows a simplified diagram of the different stress states.

The method used to produce a tension–compression stress state involves the external pressurization of the test specimen placed inside the pressure vessel, as shown in Figure 5a. The external pressure produces a hoop compression and an axial tension due to the pressure acting against the rim of the eng plugs. The stresses produced in the wall at the gauge section of the specimen are:

$$\text{axial tensile stress} = \sigma_a = \frac{P_{\text{ext}}(R^2 - r_o^2)}{(r_o^2 - r_i^2)} \tag{1}$$

$$\text{hoop compressive stress} = \sigma_h = -\frac{2P_{\text{ext}}r_o^2}{(r_o^2 - r_i^2)} \tag{2}$$

TABLE I
Theoretical Combined Stress Ratios Obtained for Plexiglas[a]

R^b in.	Stress Ratio	Pressure
2.187	−1.891	
1.812	−1.142	
1.687	−0.923	
1.562	−0.720	external pressure only
1.500	−0.625	
1.437	−0.532	
1.375	−0.445	
1.312	−0.361	
	+0.433	internal pressure only
1.500	+0.852	internal and external pressure $P_{int}/P_{ext} = 4$
2.187	−2.550	internal and external pressure $P_{int}/P_{ext} = 1/4$
1.687	−1.307	

[a] Calculated on the basis of the nominal specimen dimensions. Stress ratio = axial stress [tensile, (+)]/hoop stress [tensile, (+) or compressive (−)]; for Plexiglas, r_o = 1.000 in., r_i = 0.875 in.
[b] R = Effective radius of pressure vessel.

$$\text{stress ratio} = \frac{\sigma_a}{\sigma_h} = -\frac{R^2 - r_o^2}{2r_o^2} \tag{3}$$

where P_{ext} = pressure applied externally to the specimen; R = effective radius of the pressure vessel (i.e., internal radius of the sleeve used for any particular stress ratio); r_o = outer radius at the gauge section of the specimen; and r_i = inner radius of the specimen. By utilizing different sleeves and end plugs to alter the values of R, the tension–compression stress ratio can easily be changed.

Tension–tension stress states can be created either by internal pressurization of the closed-end test specimen (Fig. 5*b*) or by a combination of internal and external pressures (Fig. 5*c*). Only one stress ratio can be created by internal pressure (P_{int}) alone. The equations determining the stress state, in that case, are the following:

$$\text{axial tensile stress} = \sigma_a = \frac{P_{int} r_i^2}{(r_o^2 - r_i^2)} \tag{4}$$

$$\text{hoop tensile stress} = \sigma_h = \frac{P_{int}(r_o^2 + r_i^2)}{(r_o^2 - r_i^2)} \tag{5}$$

$$\text{stress ratio} = \frac{\sigma_a}{\sigma_h} = \frac{r_i^2}{(r_o^2 + r_i^2)} \tag{6}$$

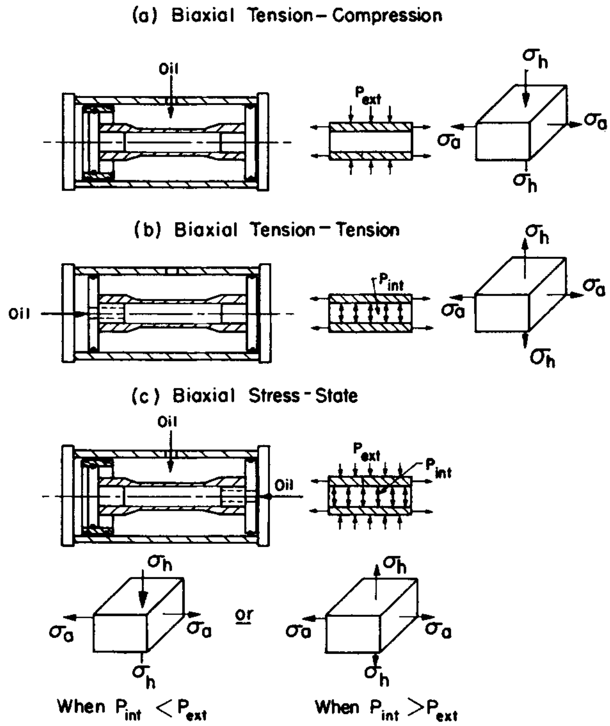

Fig. 5. Different biaxial stress states.

If the specimen is both internally and externally pressurized, either tension–tension or tension–compression stress state can be produced depending on the relative values of P_{int} and P_{ext}. If the ratio of P_{int} to P_{ext} is denoted by y, the equations for calculating the stress state at $r = r_i$ are as follows:

$$\text{axial stress} = \sigma_a = \frac{P_{ext}(R^2 - r_o^2) + yr_i^2}{(r_o^2 - r_i^2)} \tag{7}$$

$$\text{hoop stress} = \sigma_h = \frac{P_{ext}(r_o^2 + r_i^2) - 2r_o^2}{(r_o^2 - r_i^2)} \tag{8}$$

$$\text{stress ratio} = \frac{\sigma_a}{\sigma_h} = \frac{(R^2 - r_o^2) + yr_i^2}{y(r_o^2 + r_i^2) - 2r_o^2}. \tag{9}$$

When the ratio of P_{int} to P_{ext} is 4 (i.e., $y = 4$), a tension–tension stress state is created. When the ratio is 1:4, the resultant hoop stress is compressive and a tension–compression stress state is produced in the wall of the specimen.

EXPERIMENTAL PROCEDURES

Uniaxial Tensile Strength Tests

As can be seen from Figure 3, a rubber bulb must be molded to conform to the internal dimensions of the test specimen. It is seated on the conical plug and the conical plug is raised to squeeze the conical end of the rubber bulb between the conical cavity of the upper platen and the plug to achieve a seal. The upper platen is kept fixed to the test fixture by three split rings. The ring specimen is then placed on the lower platen concentrically with the rubber bulb. The lower platen is raised up into the position by a 20-ton hand pump. Spacer blocks, 2 to 3 mils higher than the ring, are placed around the specimen. The distance between the platens is kept constant during the test by closing the shut-off valve in the line. The load in the line is constantly read on a 0–24,000 lb total load gauge. Thus, the test ring in the assembled holder platens is free from any compressive restraint so that no axial force is directly applied to the specimen.

A hydraulic pump was used to generate pressure at a constant rate determined by the particular pressure command and ramp control setting on the electronic control board. The same pressure rate was used for all tests. After the air was bled from the bulb, the specimen was pressurized to failure. The pressure was read on a 0–5000 psi Heise pressure gauge and also recorded on a strip chart recorder.

After fracture, the lower platen was lowered, the fractured pieces were removed, the platens were cleaned, and the rubber bulb was cleared of debris and examined for any damage. The same rubber bulb was used for the next test if no damage was detected.

Biaxial Fracture Tests

Aluminum end plugs were adhesively bonded (epoxy-resin adhesive) to the specimen ends to form a closed cylinder. The length of the specimen ends as well as plug dimensions were determined to prevent debonding of the ends before the specimen fails. A radial clearance of approximately 0.020 in. between the plug and the internal diameter of the specimen was maintained so that there was enough adhesive between the plug and the specimen. A small step at the root of the plug can be included to keep the error due to eccentricity at a minimum. A typical end plug is shown in Figure 6.

Parker O-rings (Buna-N rubber, N219-7 series) were used for static sealing. O-ring grooves were machined on the plugs and sleeves, according to the standard recommended dimensions. The diametral clearance between two mating surfaces was 0.002 in. to 0.005 in. and the percentage squeeze (cross-section diametral compression of the O-ring between two opposite surfaces of the gland) was between 22% to 32%.

As mentioned earlier, the tension–compression stress state was created in the wall of the tube specimen by externally pressurizing the specimen. The appropriate sleeve was inserted into the pressure vessel at one end and

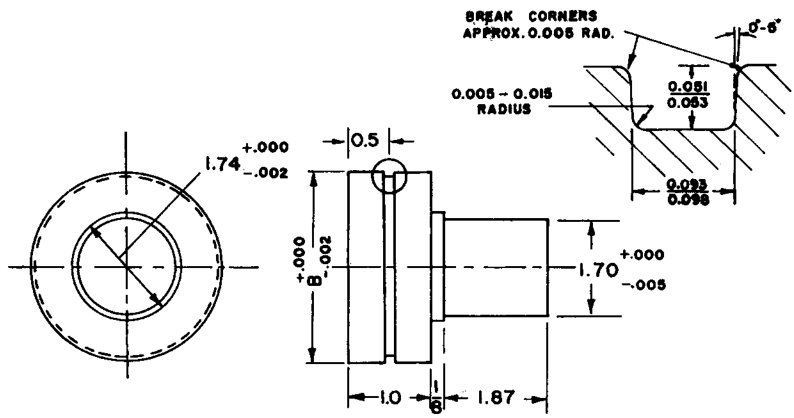

Fig. 6. End plug for Plexiglas combined stress specimens. Value of B depends on the stress ratio. Dimensions are in inches.

the specimen was then placed inside. The end plates were fastened. Air was bled from the system and a 100- to 150-psi preload was applied and maintained on the system. While bleeding the system, the specimen moved to one side of the pressure vessel (side of end plug I) owing to pressure acting on a larger area (rim) of end plug I and rested against the end plate, thus allowing the pressure to act only on the other specimen end inserted in the sleeve. The specimen was then pressurized to failure at a predetermined rate set by the ramp control and pressure command. Pressure was read on one of the Heise gauges and continuous pressure data during the test were recorded on the strip chart recorder.

The tension–tension stress states were created either by only internal pressure or by a combination of internal and external pressure. In either case, the specimen was first filled up with pressurizing oil and air was completely bled from the specimen. The rest of the procedure was the same as the tension–compression fracture test.

After the specimen fractured, the fractured surfaces of the broken specimen were removed from the pressure vessel, the vessel was cleaned, and the same procedure was repeated for other specimens. The internal and external diameters were measured, as closely as possible, at the section where fracture occurred.

RESULTS

The uniaxial tensile strength of Plexiglas was measured for 11 ring specimens. The average tensile strength of Plexiglas was 10,482 psi. The tensile strengths at different burst pressures were calculated using Lame's equation for thick cylinders. The maximum tensile stress occurs on the inside wall of the specimen and is given by

$$\sigma_{\max} = \frac{P(r_o^2 + r_i^2)}{(r_o^2 - r_i^2)} \tag{10}$$

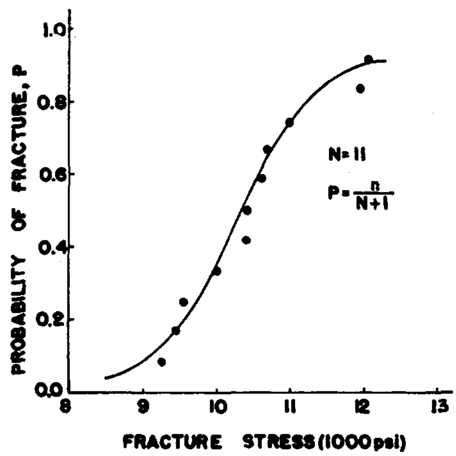

Fig. 7. Distribution of tensile stength of Plexiglas.

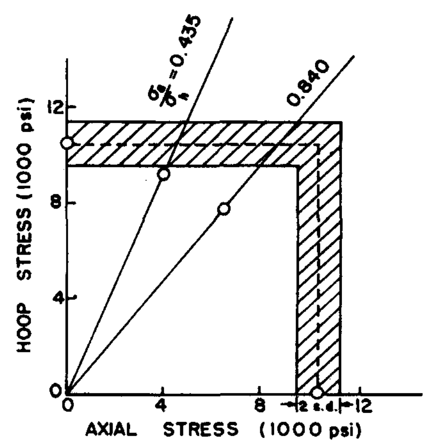

Fig. 8. Experimental tension-tension stress quadrant for Plexiglas.

The standard deviation and coefficient of variation for the uniaxial tensile strength of Plexiglas were 890 psi and 8.49%, respectively. A failure probability curve for tensile strength is shown in Figure 7.

Only two stress ratios were investigated in the tension–tension quadrant. Figure 8 compares the data to the maximum normal stress theory and the variation (standard deviation) in uniaxial tensile strength is accounted for by the shaded band. The biaxial tensile strength for Plexiglas is lower than the uniaxial tensile strength.

In the tension–compression experiments with Plexiglas, two stress ratios were created by combinations of external and internal pressures ($P_{ext} > P_{int}$) and eight stress ratios were created by external pressure only. Figure 9 shows the results obtained for Plexiglas in this stress quadrant. Here, also, the tensile strength decreases as the compressive stress in the orthog-

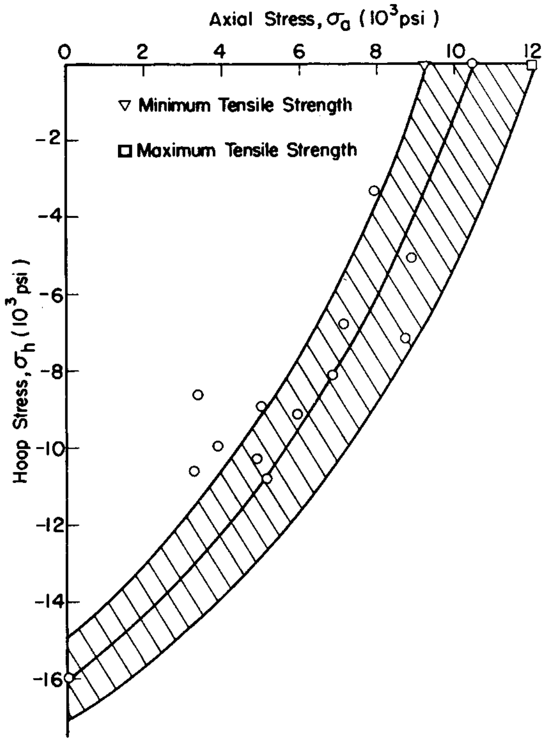

Fig. 9. Experimental tension-compression stress quadrant for Plexiglas.

onal direction increases. For comparison, the modified distortion energy theory is plotted with minimum, average, and maximum uniaxial tensile strengths used to draw a band representing the scatter in the data.

For an isotropic material under a biaxial stress system,[1] the distortion energy theory is

$$\sigma_1^2 - \sigma_1\sigma_2 + \sigma_2^2 = \sigma_{ut}^2 \tag{11}$$

where σ_1 and σ_2 are principal stresses and σ_{ut} is the ultimate tensile strength for uniaxial tension. To account for differences in compressive (σ_{uc}) and tensile strength the distortion energy theory is modified in the tension–compression stress quadrant as follows[4]

$$\left(\frac{\sigma_1}{\sigma_{ut}}\right)^2 - \frac{\sigma_1\sigma_2}{\sigma_{ut}\sigma_{uc}} + \left(\frac{\sigma_2}{\sigma_{uc}}\right)^2 = 1. \tag{12}$$

Equation (12) reduces to eq. (11) in the tension–tension quadrant. Failure envelopes constructed by means of the modified theory are discontinuous at the axes where the ratio of σ_{uc} to σ_{ut} is greater than unity.

A composite failure envelope is presented in Figure 10, along with the maximum normal stress theory, modified distortion energy theory, Cou-

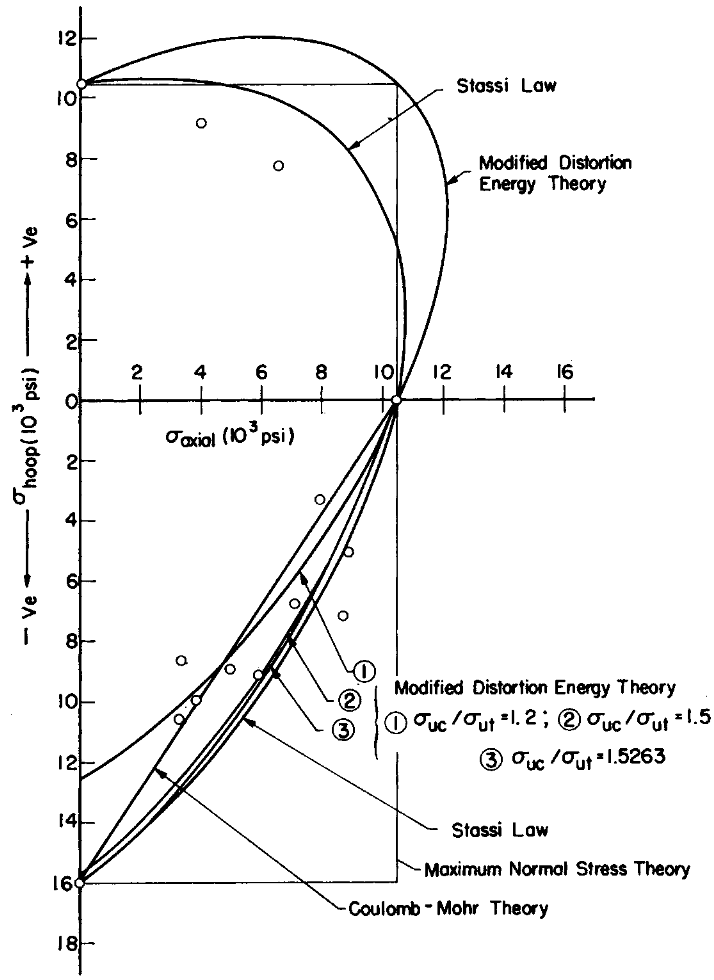

Fig. 10. Comparison of experimental data and failure criteria for Plexiglas.

lomb-Mohr theory, and Stassi law. The failure criteria were plotted using the measured compressive yield strength of Plexiglas, 16,000 psi.

In the tension–compression stress quadrant, the modified distortion energy theory fits reasonably well with the experimental data. The Stassi law[1] and modified distortion energy theory are very close to each other in the tension–compression stress quadrant. In the tension–tension stress quadrant, the Stassi law predicts a lower stress level than the modified distortion energy theory. For equal biaxial tensile stresses, the Stassi law predicts a fracture stress lower than the uniaxial fracture strength. In this stress quadrant, the experimental data do not compare well with any of the theories plotted.

CONCLUSIONS

The test method developed in this study can be used for biaxial stress experiments on brittle materials. One unique feature of this method is that the same pressure vessel can be used to generate a large number of data points in both the tension–tension and tension–compression stress quadrants.

The cylindrical test specimens with reduced sections at the center can be used to accurately determine the biaxial strengths of brittle materials.

Biaxial tension–tension and tension–compression strength results were obtained for Plexiglas. The variations in the test results can be partly attributed to the variations in the material. The biaxial tensile strength is less than the uniaxial tensile strength. The tensile strength decreases as the compressive stress in the orthogonal directions increases. For Plexiglas, the tension–compression strength data fit reasonably well with the modified distortion energy theory.

This study was supported by the U. S. Atomic Energy Commission, Contract AT (11-1)-1794, and the authors express their appreciation for this support.

References

1. R. E. Ely, *Combined Stress Properties for Acrylic Tube Specimens*, Report No. (RR-TR-64-15), U.S. Army Missile Command, Redstone Arsenal, Ala., August 1964.

2. R. Sedlacek and F. A. Halden, *Rev. Sci. Instrum.*, **33**, 298 (1962).

3. S. Timoshenko, *Strength of Materials*, Part 2, ed. 3, D. Van Nostrand, Princeton, N. J., 1956.

4. J. C. Fisher, ASTM Bulletin, No. 181, April 1952, p. 74

Received February 17, 1970
Revised March 30, 1970